BCI Monitor Enhances Electroencephalographic and Cerebral Hemodynamic Activations During Motor Training

Zhongpeng Wang, Yijie Zhou, Long Chen, Bin Gu, Weibo Yi, Shuang Liu, Minpeng Xu, *Member, IEEE*, Hongzhi Qi, *Member, IEEE*, Feng He, and Dong Ming, *Senior Member, IEEE*

***Abstract*— Motor imagery-based brain-computer interface (MI-BCI) controlling functional electrical stimulation (FES) is promising for disabled patients to restore their motor functions. However, it remains unclear how much the BCI part can contribute to the functional coupling between the brain and muscle. Specifically, whether it can enhance the cerebral activation for motor training? Here, we investigate the electroencephalographic and cerebral hemodynamic responses for MI-BCI-FES training and MI-FES training, respectively. Twelve healthy subjects were recruited in the motor training study when concurrent electroencephalography (EEG) and functional near-infrared spectroscopy (fNIRS) were recorded. Compared with the MI-FES training conditions, the MI-BCI-FES could induce significantly stronger event-related desynchronization (ERD) and blood oxygen response, which demonstrates that BCI indeed plays a functional role in the closed-loop motor training. Therefore, this paper verifies the feasibility of using BCI to train motor functions in a closed-loop manner.**

***Index Terms*— Brain-computer interfaces, motor training, functional electrical stimulation, blood oxygen response, event-related desynchronization.**

I. Introduction

BRAIN-COMPUTER interfaces (BCIs) provide users with a direct communication pathway between the brain and the outward environment, which are a promising approach for disabled patients to replace or rehabilitate their motor functions [1]. Specifically, motor imagery-based BCI (MI-BCI) detects the body movement intents and transfer them into command orders to control outside devices [2], [3]. Recent studies have shown that MI-BCI linked with functional electric stimulation (FES) or assistive devices could couple the activities between the brain and muscle, thereby improving motor training performance and even restoring the stroke patient's motor ability [4].

To our knowledge, MI could bring about similar neural activations in sensorimotor cortical areas with real movement, which could affect motor learning ability and functional neuroplasticity [5]. Nakayashiki *et al.* [6] demonstrated both MI training and real motor execution training could activate specific motor areas and improve the behavior performance. Additionally, MI combined assistive device could further enhance brain activity patterns by reconstructing functional pathway for the affected limb [7]. Qiu *et al.* [8] also proposed a FES induced lower limb movement pattern and quantitatively demonstrated its β band event-related desynchronization/ synchronization (ERD/ERS) patterns were similar to active movement. Compared to the baseline before training, patients with stroke showed significant differences in sensorimotor cortex after several sessions of MI based BCI-FES training [9], [10]. After MI-BCI training, patients with spinal cord injury (SCI) had a comparable cortical activation in the motor area with the healthy people [11].

To evaluate the brain functional activation, multichannel functional near-infrared spectroscopy (fNIRS) and EEG have been widely used in the neuroscience community [12]–[15]. As non-invasive brain imaging techniques, the two methods could be easily combined and have the advantage of complementing to each other with different brain signal patterns [16]–[20]. Therefore, as a novel supplement of the conventional EEG signals, the fNIRS could be quantified by the oxygenated and deoxygenated hemoglobin ([oxy-Hb]/[deoxy-Hb] or HbO/HbR) [21], [22]. Fazli *et al.* [12] have preliminarily demonstrated the feasibility of a hybrid NIRS-EEG approach to enhance BCI performance .

Previous studies also showed a novel method to simultaneously acquire the fNIRS and EEG signals from the sensorimotor area [12], [23]. V. Kaiser *et al.* demonstrated BCI based motor neurofeedback training for several sessions could change brain network patterns and significantly enhance the motor cortical excitability. These effects could be effectively quantified by multiband ERD patterns

Manuscript received October 6, 2018; revised January 27, 2019; accepted March 3, 2019. Date of publication March 7, 2019; date of current version April 8, 2019. This work was supported in part by the National Key Research and Development Program of China under Grant 2017YFB1300302, in part by the National Natural Science Foundation of China under Grant 81630051, Grant 91648122, Grant 81601565, and Grant 61603269, and in part by the Tianjin Key Technology R&D Program under Grant 17ZXRGGX00020 and Grant 16ZXHLSY00270. *(Corresponding authors: Long Chen; Dong Ming.)*

Z. Wang, B. Gu, M. Xu, H. Qi, and F. He are with the College of Precision Instruments & Optoelectronics Engineering, Tianjin University, Tianjin 300072, China.

Y. Zhou and S. Liu are with the Academy of Medical Engineering and Translational Medicine, Tianjin University, Tianjin 300072, China.

L. Chen and D. Ming are with the College of Precision Instruments & Optoelectronics Engineering, Tianjin University, Tianjin 300072, China, and also with the Academy of Medical Engineering and Translational Medicine, Tianjin University, Tianjin 300072, China (e-mail: cagor@tju.edu.cn; richardming@tju.edu.cn).

W. Yi is with the Beijing Institute of Mechanical Equipment, Beijing 100854, China.

Digital Object Identifier 10.1109/TNSRE.2019.2903685

in EEG and hemodynamic responds in fNIRS [23], [24]. Biasiucci *et al.* [9] proposed a BCI-actuated FES training approach eliciting remarkable effects of lasting arm motor recovery after stroke. However, it still short of comprehensive investigation to evaluate how much the BCI part can contribute to the functional coupling between the brain and muscle during motor training [25]. The correlations between the EEG and fNIRS features for BCI based motor training have not been quantitatively discussed a lot.

This work aims to evaluate the effects of BCI based motor training and how the cortical activations of sensorimotor cortex changes over different motor training conditions. To this end, a scalp EEG and fNIRS based experimental paradigm was conducted. It contained four different training conditions (i.e. MI-BCI-FES, MI-FES, MI and FES). The results of twelve healthy participants showed the MI-BCI combined FES could induce significantly stronger cortical activations than others according to the overall ERD patterns of EEG and the hemodynamic responses of fNIRS. Additionally, there were significant correlations between the ERD patterns and hemodynamic responses. These results could quantitatively evaluate electroencephalographic and cerebral hemodynamic activations and verify the feasibility of closed-loop BCI monitor during motor neurofeedback training.

II. Methods

A. Participants

Twelve right-handed healthy volunteers (five females, mean age 21.5 ± 1.5, range 20 to 25 years old) participated in this study. All participants stated that they have no history of neurological or psychiatric disorders. The experimental procedure was clearly explained to each participant and a written informed consent was also obtained before data recording. This study was approved by the ethical committee of Tianjin University before the experiments.

B. Design of the Experimental Paradigm

To probe the effects of BCI monitor during motor training, ten sessions in total were conducted, including two calibration sessions, and two sessions for each motor training conditions (MI-BCI-FES, MI-FES, MI and FES). The interval between these different training conditions were 1–3 days. In each session, participants were seated comfortably in an armchair in front of a 27-inch screen with 1 meter distance. The first two sessions were used to calibrate the BCI system and get the participants familiar with MI. After that, the four different training conditions were conducted in a random order.

Fig. 1(a) illustrates the experimental paradigm for calibration sessions. The participants were asked to imagine kinesthetic grasping movement of the right hand (RH MI) or keep relaxed. Each session consisted of 40 trials (20 for RH MI, 20 for Relax). One trial lasted 5 s. At the beginning of a trial, a white circle appeared in the middle of the screen and stayed for the preparation of the trial. After 1s, a cue in the form of a white cross with or without arrow appeared for 4 s, indicating the participants should perform RH MI or keep

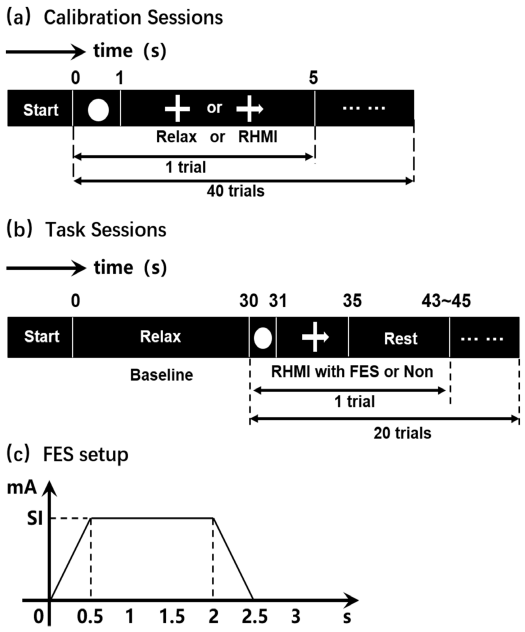

Fig. 1. Experimental paradigm. (a) The calibration trial structure. Each trial started with a white circle, followed by a white cross with or without arrow appeared for 4 s. The arrow cued the participants to perform the indicated task for 4 s. (b) Trial structure for four tasks. At the beginning of each session, 'Relax' indicated a 30 s relaxation for the baseline. Each trial started with a white circle, followed by a white cross with arrow appeared for 4 s. 'Rest' indicates an 8∼10 s random rest before the next trial. (c) FES started 0 second to 2.5 second as one FES feedback. SI indicates stimulation intensity individually determined.

relaxed as long as the fixation cross was on the screen. Then the fixation cross disappeared and the screen became blank for a random interval between 3 and 4 s. Participants were asked to avoid electromyogram artifacts by restricting movements like eye blinking or swallowing during the task period.

The two calibration sessions' EEG data (40 trials of Relax and 40 trials of MI) in the epoch from 0.5 to 3.5 s after task cue onset were extracted and used to construct the common spatial pattern (CSP) and a radial basis function (RBF) kernel support vector machine (SVM) classifier, which had been proved with a relatively high classification performance using the LIBSVM toolbox [26]. Fig. 1(b) illustrates the experimental paradigm for task sessions of the four different conditions, in which the participants were given different feedback. Each session consisted of 20 trials. And each trial lasted 5 s. At the beginning of each trial, a white circle appeared in the middle of the screen and stayed for preparation of the trial. After 1s, a task cue in the form of a white cross with arrow appeared for 4 s. Then the cue cross disappeared and the screen became blank for a random time interval between 8 and 10 s.

For the MI-BCI-FES sessions, the participants were asked to imagine kinesthetic grasping movement of the right hand as they did in the calibration sessions. The FES would be triggered to realize the hand grasping movement if the BCI classifier recognized a motor imagery of right hand during the task period of each trial. The FES was performed using VitalStim therapy (Chattanooga Group, TN, USA), which could deliver a constant current. The stimulation waveform was 30 Hz with a series of 300μs biphasic pulses. The FES parameters and electrodes were setup as shown in Fig. 1(c)

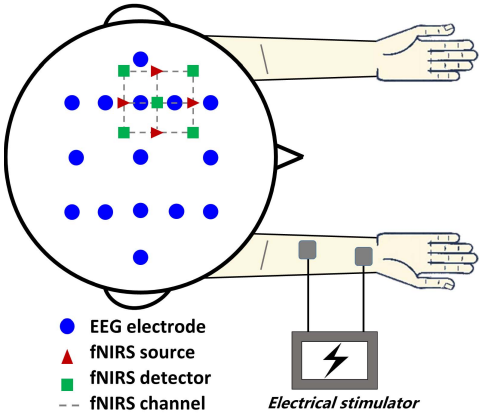

Fig. 2. 15 electrodes positions (shaded in blue dots) were used for EEG recording. The red triangles denote the source probes, the green squares denote the detectors probes, and the gray dashed lines denote the fNIRS optical channels for continuous 12-channel hemodynamic responses recording. The standard FES electrodes were about 10cm apart placed at the right wrist and middle position of the forearm.

and Fig. 2. The MI-FES sessions had the same paradigm with MI-BCI-FES sessions but had no BCI controls. FES feedback was applied randomly in MI period. For MI sessions, the participants were asked to imagine kinesthetic grasping movement of the right hand like the calibration sessions. There was no BCI control and FES feedback. For FES sessions, the participants were asked to relax. A FES feedback was applied randomly during the task period of each trial.

C. EEG Recording and Processing

EEG data were acquired by a SynAmps2 system (Neuroscan, Australia) with standard Ag/AgCl electrodes placed on the scalp according to the international 10/20 system. For the EEG based BCI control, 15 selected electrodes (labeling F3, FZ, F4, FC3, FC4, C5, C3, CZ, C4, C6, CP3, CP4, P3, PZ, P4 as shown in Fig. 2) were mounted in both horizontal and vertical directions covering the sensorimotor cortex. The reference electrode was placed on the nose and the ground electrode was placed on the forehead. EEG signals were band-pass filtered between 0.5 and 100 Hz and sampled at 1000 Hz. A notch filter with 50 Hz was used during the data acquisition. For the preprocessing, the EEG raw data were downsampled at 200 Hz, then processed by the common average reference (CAR).

The averaged event-related power changes in a time-frequency domain could be visualized by the event-related spectral perturbation (ERSP), which provides detailed information for ERD/ERS patterns of different tasks. An ERSP of n trials was calculated according to equation defined as follows:

$$ERSP(f,t) = \frac{1}{n}\sum_{k=1}^{n}(F_k(f,t)^2) \tag{1}$$

where $F_k(f,t)$ indicates the spectral estimation at frequency f and time t for the kth trial. The ERSP (dB) was computed through short-time Fourier transform (STFT) with a 256 points Hanning-tapered window from EEGLAB [26]. For the baseline-normalized ERSP, the mean power changes in a baseline period (the 1 s epoch before task cue) were subtracted from each spectral estimation. In this work, the ERSP from two key electrodes C3 and C4 were displayed from -1 to 6 s between 5 and 35 Hz. Additionally, we calculated the absolute $\alpha-$ERD (8–13 Hz) and $\beta-$ERD (14–29 Hz) of all EEG channels with its topographical distributions according to the method of baseline-normalized ERSP, which could indicate the cortical electrophysiological activations.

Moreover, to quantitatively investigate the ERD patterns for different motor training conditions, we calculated the relative ERD power (RP_{ERD}) across all participants using the P_n according to equation defined as follows [7]:

$$P_{relax} = \frac{1}{T_{relax}}\sum_{n\in T_{relax}} P_n \tag{2}$$

$$P_{\text{task}} = \frac{1}{T_{\text{task}}}\sum_{n\in T_{\text{tesk}}} P_n \tag{3}$$

$$RP_{ERD} = \frac{P_{\text{task}} - P_{\text{relax}}}{P_{\text{relax}}} \times 100 \tag{4}$$

where P_{relax} and P_{task} are the average power spectra during the rest period (T_{relax}) and the task period (T_{task}). RP_{ERD} was averaged across trials within a participant. The salient $\alpha-$ERD (8–13 Hz) and wide $\beta-$ERD (14–29 Hz) were also selected respectively. The relative $\alpha/\beta-$ERD power of each single participant were also proposed to indicate the relatively consistent trend across all participants.

D. fNIRS Recording and Processing

A multi-channel oxygenation monitor (NirScan, Danyang Huichuang Medical Equipment Co. Ltd.) was used to record the hemodynamic responses of the participants over the four different training conditions. The probes were positioned over left sensorimotor cortex area (SMA) as shown in Fig. 2. The distance between sources and detectors was 3 cm. The sampling rate was set to 20 Hz.

The anti-correlation between [oxy-Hb] and [deoxy-Hb] based method was utilized to evaluate and improve the fNIRS raw data quality [27]. The oxy- and deoxy-Hb are negatively correlated when noise level is low. When noise level increases, their correlation becomes more and more positive. Assume the measured signal has four components: Let x, y, x_0 and y_0 be measured [oxy-Hb], [deoxy-Hb], true [oxy-Hb], and true [deoxy-Hb], then

$$\begin{aligned} x &= x_0 + pF + \text{Noise} \\ y &= y_0 + F + \text{Noise} \end{aligned} \tag{5}$$

where F is noise which has identical effects on [oxy-Hb] and [deoxy-Hb] to a positive constant factor p. The "Noise" term in the equation is usually high frequency white noise introduced by the fNIRS device. The goal is to find x_0 and y_0 subject to two assumptions: 1) x_0 and y_0 should be maximally negatively correlated (close to -1). 2) x_0 and F should be minimally correlated (close to 0). Assume assumption 1) is satisfied, we can express the relationship between

x_0 and y_0 as

$$x_0 = -qy_0 \tag{6}$$

where q is a free parameter accounting for the amplitude difference between [oxy-Hb] and [deoxy-Hb]. By inserting *eq.*(6) to *eq.* (5), then

$$\begin{aligned} F &= (x + qy)/(p + q) \\ x_0 &= q(x - py)/(p + q) \end{aligned} \tag{7}$$

Then we apply the second assumption that F and x_0 should be minimally correlated. If we set the correlation between $F$and $x_0$to zero, then we get

$$\sum_t x^2 + (q - p)\sum_t xy - pq\sum_t y^2 = 0 \tag{8}$$

The assumption is justified by the fact that the resultant method is efficient at removing head motion induced noise. With $p = q$, Thus we reach a very simple result,

$$\begin{aligned} x_0 &= (x - py)/2 \\ y_0 &= -x_0/p \end{aligned} \tag{9}$$

where $p$is the ratio of the standard deviation of measured [oxy-Hb] and [deoxy-Hb] signal. We used a window of 100 s to calculate $p$coefficient. According to this principle, none or not more than two bad-channels data was removed over all participants. And then during the preprocessing, the raw data were band-pass filtered between 0.01 and 0.2 Hz. The moving average methods was used to remove the outlier terms in the fNIRS data. The averaged task-related changes of [oxy-Hb], [deoxy-Hb] and [total-Hb] referred to a 2 s baseline interval prior to the task trial were calculated for each fNIRS channel. Additionally, the hemodynamic responses of the four motor training conditions across all participants were also averaged at the regions of interest (ROI) channels around the C3 [23], [28].

Moreover, we calculated the topographical distributions of hemodynamic responses according to the averaged task-related changes of [oxy-Hb], [deoxy-Hb] and [total-Hb], which could indicates the cortical hemodynamic activations. To quantitatively investigate the task-related changes of the averaged [oxy-Hb] and [deoxy-Hb] hemodynamic responses over the four conditions, three parameters were calculated including peak amplitude, peak latency and integral area according to the averaged hemodynamic curves.

E. Statistical and Correlations Analysis

In view of the overall electroencephalographic and cerebral hemodynamic responses during different motor training conditions, The relative ERD powers and fNIRS feature parameters (i.e. peak amplitude, peak latency and integral area) between different conditions were analyzed by one-way repeated measures analysis of variance (ANOVA), a widely used statistical test method in EEG and fNIRS parameters [24], [26], [28], with the motor training conditions as an independent factor and relative ERD or hemodynamic parameters as a within-subject factor. These tests were performed with SPSS 22.0 (IBM SPSS Inc., Chicago, IL, USA) in this work.

Additionally, in view of the relatively consistent spatial distributions over left SMA around the C3 channel, correlation analysis of the relative ERD powers and fNIRS feature parameters was tested by a 2-tailed Pearson correlation test based on twelve participants by four conditions (i.e. forty-eight values) in order to obtain the relationships between electrophysiological and hemodynamic responses.

III. Results And Analysis

A. Event-Related Spectral Perturbation (ERSP)

Fig. 3(a) shows the averaged ERSP at electrodes C3 and C4 for MI-BCI-FES, MI-FES, MI and FES task conditions. The topographical distribution maps are also shown across all participants. The time-frequency maps present a long-lasting $\alpha-$ERD (8–13 Hz) and $\beta-$ERD (14–29 Hz) from task onset for all four conditions, especially clear for MI-BCI-FES. The averaged topographical spatial distributions of absolute $\alpha/\beta-$ERDs were also proposed obtaining a consistent phenomenon. Laterality of cortical activations was clearer for the MI-BCI-FES conditions.

To quantitatively verify the effectiveness of BCI monitor in the closed-loop motor training, the wide $\alpha-$band from 8 to 13 Hz and $\beta-$band from 14 to 29 Hz were selected respectively to compare their relative ERD powers over all conditions. Fig. 3(b) shows the averaged relative $\alpha/\beta-$ERD powers across all participants of C3 channel. One-way repeated measures ANOVA yielded significant differences of $\alpha-$ERD ($F(2.426, 26.690) = 5.402$, $p = 0.008 < 0.01$) and $\beta-$ERD ($F(1.791, 19.698) = 24.104$, $p = 0.000 < 0.001$) with Huynh-Feldt correction across the four different training conditions. Besides, the Bonferroni post hoc test yielded significant differences of $\alpha-$ERD (MI-BCI-FES vs. FES: $p = 0.012$, MI-FES vs. FES: $p = 0.037$) and $\beta-$ERD (MI-BCI-FES vs. MI: $p = 0.000$, MI-BCI-FES vs. FES: $p = 0.000$, MI-FES vs. MI: $\mathrm{p} = 0.003$, MI-FES vs. FES: $p = 0.006$) with pairwise comparisons. The relative $\alpha/\beta-$ERDs of each single participant were also proposed, which could indicate the relatively consistent trend, especially significant for MI-BCI-FES at the relative $\beta-$ERD power, so that BCI indeed plays a crucial role in the closed-loop motor training.

B. EEG Based Classification Performance

As aforesaid, the common spatial pattern (CSP) and support vector machine (SVM) algorithm were applied to calculate the classification accuracies of the calibration and motor training conditions (i.e. MI-BCI-FES, MI-FES and MI, as FES condition had no motor imagery involved). Classification results of the calibration sessions (40 trials) were estimated using a leave-one-out paradigm. And the other conditions (40 trials each) except the FES were calculated using an online paradigm based on the calibration sessions' classifier. As shown in TABLE I, The averaged classification performance of all the motor training conditions is over 80%. Except calibration sessions, the MI-BCI-FES achieves a relatively higher online

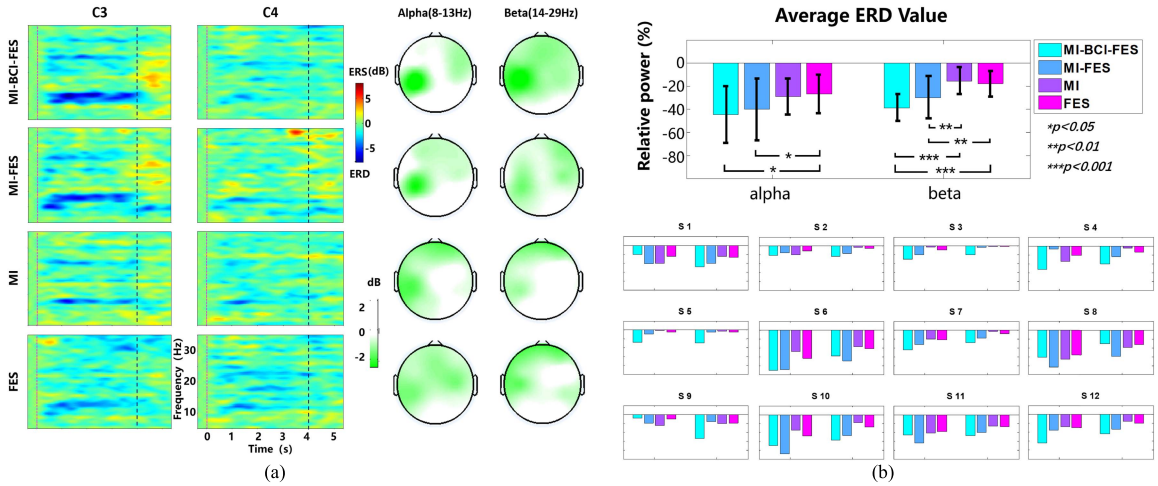

Fig. 3. ERSP results of the four different task conditions. (a) Averaged time-frequency maps across all participants. The red dashed lines indicate the onset and the black dashed lines offset of the task-related period. C3 and C4 are the key EEG channels for laterality analysis. Averaged topographical distributions of absolute alpha-ERD (8–13 Hz) and beta-ERD (14–29 Hz) were also proposed to indicate cortical activation differences over the different conditions. (b) Averaged relative alpha/beta-ERD power of C3 EEG channel. And the relative alpha/beta-ERD power of each single participant were also proposed to indicate the relatively consistent trend across all participants.

TABLE I
CLASSIFICATION PERFORMANCE OF DIFFERENT CONDITIONS

Subject	Classification Accuracy (%)			
	Calibration	*MI-BCI-FES*	*MI-FES*	*MI*
S1	80.00	80.00	75.00	80.00
S2	75.00	82.50	72.50	82.50
S3	87.50	82.50	77.50	77.50
S4	75.00	65.00	80.00	85.00
S5	80.00	87.50	82.50	87.50
S6	97.50	92.50	87.50	90.00
S7	72.50	72.50	85.00	70.00
S8	97.50	95.00	90.00	87.50
S9	82.50	90.00	82.50	72.50
S10	90.00	75.00	85.00	75.00
S11	90.00	82.50	80.00	82.50
S12	85.00	75.00	75.00	72.50
Mean	84.38	81.67	81.04	80.21
Std.	8.40	8.81	5.38	6.70

classification performance than the other conditions although there is no significant difference.

C. Cerebral Hemodynamic Responses of the fNIRS

For the overall cortical effects analysis. Fig. 4(a) shows the averaged cerebral hemodynamic responses of MI-BCI-FES, MI-FES, MI and FES conditions at the ROI channels around the C3 across all participants. The wave curves present a relatively consistent trend which first ascends during the task period and then descends to the baseline during the rest period. We can see that the MI-BCI-FES condition could induce the clearest hemodynamic responses relatively to the other three conditions.

As shown in Fig. 4(b), the peak amplitude, peak latency and integral area were calculated according to the averaged cerebral hemodynamic curves. For statistical difference analysis, ANOVA was also conducted in the [oxy-Hb], which is the key parameter of hemodynamic responses reflecting the cortical activations. The results yielded significant differences in the peak amplitude ($F(2.030, 22.328) = 6.636$, $p = 0.005 < 0.01$), peak latency ($F(3, 33) = 4.533$, $p = 0.009 < 0.01$) and integral area ($F(1.772, 19.489) = 10.529$, $p = 0.001 < 0.01$) with Huynh-Feldt correction across the four different training conditions. Besides, the Bonferroni post hoc test yielded significant differences between conditions in the peak amplitude (MI-BCI-FES vs. FES: $p = 0.034$), peak latency (MI-BCI-FES vs. FES: $p = 0.014$) and integral area (MI-BCI-FES vs. MI-FES: $p = 0.043$, MI-BCI-FES vs. MI: $p = 0.023$, MI-BCI-FES vs. FES: $p = 0.016$) with pairwise comparisons, which indicates the BCI in closed-loop motor training could produce stronger cerebral hemodynamic activations than the other three conditions.

In addition, Fig. 5 shows the averaged topographical distributions of cerebral hemodynamic activations over different conditions, including the [oxy-Hb], [deoxy-Hb] and [total-Hb] responses of the ROI around the C3 across all participants. The topographical maps of hemodynamic responses could obviously reflect cortical activation over the ROI. The results indicate it is similar for spatial distributions of hemodynamic patterns with circumscribed right hand motor cortical activations for these four task conditions. Especially, the MI-BCI-FES condition produces the clearest hemodynamic responses relatively to the other three conditions, which demonstrates that BCI control plays a functional role in the motor training.

D. Correlation Analysis Between ERD Patterns and fNIRS Features

Due to the similarity of relative ERD powers and fNIRS features during the four different motor training conditions,

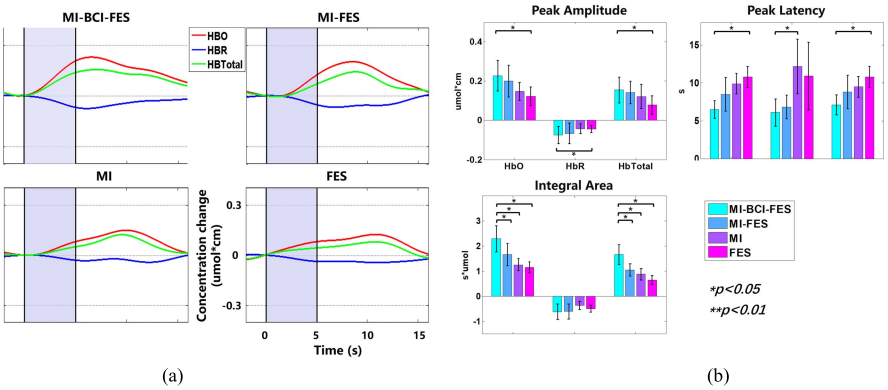

Fig. 4. Averaged hemodynamic responses. (a) Averaged changes in the [oxy-Hb], [deoxy-Hb] and [total-Hb] responses of the ROI fNIRS channels around the C3. The black lines indicate the onset and offset of the task period. (b) Averaged three parameters including peak amplitude, peak latency and integral area for the different task conditions.

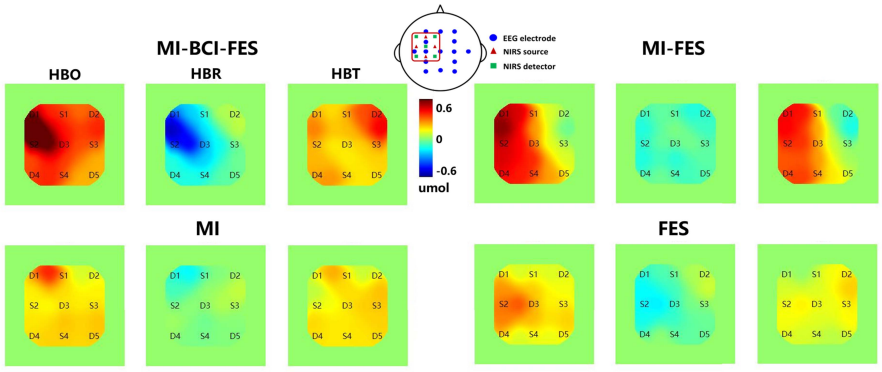

Fig. 5. Averaged topographical distributions of hemodynamic responses over different conditions, including the [oxy-Hb], [deoxy-Hb] and [total-Hb] responses of the ROI around the C3. The red and blue colors indicate high and low hemodynamic activations respectively.

correlation analysis was employed to verify whether there are significant relationships or consistent trends between electroencephalographic and cerebral hemodynamic activations of the ROI around the C3. As shown in Fig. 6, The correlation analysis yielded significant relationships between ERD patterns and fNIRS features: $\alpha-$ERD and peak amplitude ($r = -0.4386, p = 0.0018$), $\alpha-$ERD and integral area ($r = -0.4594, p = 0.0010$), $\beta-$ERD and peak amplitude ($r = -0.4392, p = 0.0018$), $\beta-$ERD and integral area ($r = -0.4473, p = 0.0014$), while there is no significant relationship between the other two pairs (i.e. $\alpha-$ERD and peak latency:$r = 0.2207$, $p = 0.1318$, $\beta-$ERD and peak latency: $r = 0.2379$, $p = 0.1035$). These results indicate that the relationships between ERD patterns and cerebral hemodynamic features which present a relatively consistent trend might be quantified through above method and it is a promising approach combining electrophysiology and hemodynamic responses to evaluate the effectiveness of motor training.

IV. Discussion

In previous researches, Khan *et al.* [29] and Fu *et al.* [30] have showed the hybrid NIRS-EEG technology could achieved a high classification performance for complex motor imagery patterns, i.e. different directions of limb movement or different imagined hand clenching force and speed. In this work, the simple motor imagery based 2-class BCI task have no difficult for all the participants to achieve a relatively high classification performance, which also could be proved by the topographical distributions of ERD as shown in Fig. 3(a) and hemodynamic responses as shown in Fig. 5. The averaged classification performance of all the motor training conditions is over 80%. Except calibration sessions, the MI-BCI-FES achieves a relatively higher online classification performance relative to the other conditions and there is no significant difference. However, the performance is not a crucial discussion point but the effectiveness of closed-loop BCI based motor training in our study.

Therefore, at the beginning of this study, we would like to investigate whether BCI monitor could effectively enhances electroencephalographic and cerebral hemodynamic activations during motor training? We have considered there should be significant increases in ERD patterns and cerebral hemodynamic responses for MI-BCI-FES relative to the other conditions. The significant differences were obviously visible between MI-BCI-FES and MI or FES conditions. Specifically, It was significant in cerebral hemodynamic responses between MI-BCI-FES training and MI-FES training but not significant in ERD patterns. A possible explanation was that the dif-

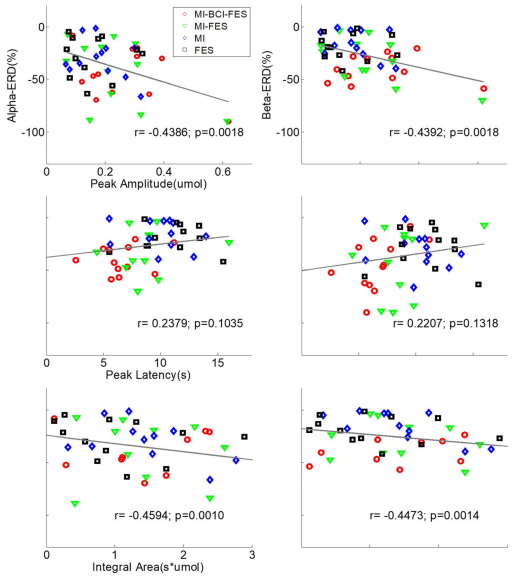

Fig. 6. Correlation analysis between relative alpha-, beta-ERD power of EEG features and peak amplitude, peak latency, integral area of fNIRS features for all the participants.

ferent motor training conditions could elicit a relatively high performance as shown in TABLE I and consistent electroencephalographic effects but different cerebral hemodynamic activations as shown in Fig. 3 ∼ 5. Therefore, some more complex patterns of motor imagery should be involved for further research [29].

For correlations analysis, V. V. Nikulin *et al.* have investigated Monochromatic Ultra-Slow (∼ 0.1 Hz) Oscillations (MUSO) in the human electroencephalogram and their correlations with hemodynamic responds. The results showed a coherence between MUSO and NIRS features. Moreover, different electrode sites demonstrated the coherence was not reducible to volume conduction. MUSO were unlikely to be generated by one source. They suggested that these oscillations might be of a rather extra neuronal origin reflecting cerebral vasomotion [31]. While there is no more research for the correlations between cerebral hemodynamic responses and αor $\beta-$ERD patterns [32]. E. Visani *et al.* focused on the functionally activated area maximizing the useful information instead of preselected structural areas. This work found not only the typical EEG pattern distinguishing patients with cortical myoclonus from controls (almost absent $\beta-$ERS), but also significant differences in the BOLD and fNIRS features, both of which were significantly reduced. The cerebral hemodynamic activations revealed by fMRI and fNIRS were consistent in the patients and controls, thus indicating that both methods were similarly capable to identify the neurovascular changes occurring during a motor task under physiological and pathological conditions [15]. The cortical effects of motor training in a MI-BCI proposed by Kaiser *et al.* [23] showed an [oxy-Hb] increase in fNIRS and a stronger upper $\beta-$ERD in the EEG especially in users with low BCI performance. MI-related operant learning of brain self-regulation is facilitated by proprioceptive feedback and mediated in the sensorimotor $\beta-$band [33].

Differing from previous studies [15], [23], [31], [32], the primary goal of this study was to investigate and compare the cortical activations during different motor training conditions measured by fNIRS and EEG. The correlations between EEG and fNIRS features were also discussed. There were significant relationships between ERD patterns and fNIRS features (i.e. $\alpha-$ERD and peak amplitude, $\alpha-$ERD and integral area, $\beta-$ERD and peak amplitude, $\beta-$ERD and integral area), while there is no significant relationship between the other two pairs (i.e. $\alpha-$ERD and peak latency, $\beta-$ERD and peak latency) as shown in Fig. 6. These results indicated that the relationships between ERD patterns and cerebral hemodynamic features might be quantified through above method and it might be a promising approach combining electrophysiology and hemodynamic responses to evaluate the effectiveness of motor training. The features in EEG and fNIRS have relatively consistent trend in a statistical level.

Furthermore, previous studies for the motor neurofeedback training technology have proved it is available for motor ability or functional neuroplasticity improvement to combine BCI with some outside devices [34]–[36]. Boe *et al.* [37] found that MI-related brain activations increased in contralateral sensorimotor cortex after the imagined movement across sessions in the neurofeedback group, but not in control group. During neurofeedback training, fNIRS combined with EEG had advantages to classify different brain states by benefiting from the complementary information [12], [29]. Additionally, Miller *et al.* [38] demonstrated MI induced cortical activations were significantly augmented, even exceeding that of overt movement focusing on oscillation powers in high frequency (76–100 Hz) and low frequency (8–32 Hz) bands . Some promising feature extraction algorithms and visual stimuli paradigms were also proposed to optimize BCI manner [39], [40]. Nevertheless, more kinesthetic devices such as FES have been involved in the close-loop BCI based motor training nowadays. Therefore, this work aims to compare these motor training conditions according to the electroencephalographic and cerebral hemodynamic activations. It also demonstrated the presence of the coherence between EEG oscillations at wide α and β frequency band and cerebral hemodynamic patterns of fNIRS. The overall results provided a promising relatively portable measurement to quantitatively evaluate the effectiveness of BCI training and verify the MI-BCI-FES framework could contribute a foundation for motor neural rehabilitation system. For the future research, in view of the limitation of EEG and fNIRS channels, there should be more probes with origin source analysis through the whole brain measurement.

V. Conclusion

This work investigated the effectiveness of closed-loop BCI monitor during motor training from the view of EEG and cerebral hemodynamic activations. All these findings obtained in this study indicated that MI-BCI combined FES achieved a larger cortical activation relative to the other conditions according to the electrophysiology and hemodynamic responses. Besides, the significant correlations between

relative ERDs and hemodynamic responses for these motor training conditions were also discussed, which might be an available evaluation method for motor rehabilitation applications. Therefore, closed-loop BCI based motor training measured by fNIRS and EEG prospectively provides an available approach for motor rehabilitation and neurofeedback training research.

ACKNOWLEDGMENT

The authors sincerely thank all participants for their voluntary participation.

REFERENCES

[1] F. Pichiorri *et al.*, "Brain-computer interface boosts motor imagery practice during stroke recovery," *Ann. Neurol.*, vol. 77, no. 5, pp. 851–865, Mar. 2015.

[2] M. Ietswaart *et al.*, "Mental practice with motor imagery in stroke recovery: Randomized controlled trial of efficacy," *Brain*, vol. 134, no. 5, pp. 1373–1386, May 2011.

[3] M. A. Dimyan and L. G. Cohen, "Neuroplasticity in the context of motor rehabilitation after stroke," *Nature Rev. Neurol.*, vol. 7, no. 2, pp. 76–85, Feb. 2011.

[4] M. Takahashi, K. Takeda, Y. Otaka, R. Osu, and T. Hanakawa, "Event related desynchronization-modulated functional electrical stimulation system for stroke rehabilitation: A feasibility study," *J. Neuroeng. Rehabil.*, vol. 9, no. 1, p. 56, Dec. 2012.

[5] R. Sitaram *et al.*, "Closed-loop brain training: The science of neurofeedback," *Nature Rev. Neurosci.*, vol. 18, no. 2, pp. 86–100, Feb. 2017.

[6] K. Nakayashiki, M. Saeki, Y. Takata, Y. Hayashi, and T. Kondo, "Modulation of event-related desynchronization during kinematic and kinetic hand movements," *J. Neuroeng. Rehabil*, vol. 11, no. 1, p. 90, Dec. 2014.

[7] W.-K. Tam, K.-Y. Tong, F. Meng, and S. Gao, "A minimal set of electrodes for motor imagery BCI to control an assistive device in chronic stroke subjects: A multi-session study," *IEEE Trans. Neural. Syst. Rehabil. Eng.*, vol. 19, no. 6, pp. 617–627, Dec. 2011.

[8] S. Qiu *et al.*, "Event-related beta EEG changes during active, passive movement and functional electrical stimulation of the lower limb," *IEEE Trans. Neural. Syst. Rehabil. Eng.*, vol. 24, no. 2, pp. 283–290, Feb. 2016.

[9] A. Biasiucci *et al.*, "Brain-actuated functional electrical stimulation elicits lasting arm motor recovery after stroke," *Nature Commun.*, vol. 9, no. 1, Jun. 2018, Art. no. 2421.

[10] B. M. Young *et al.*, "Changes in functional brain organization and behavioral correlations after rehabilitative therapy using a brain-computer interface," *Front. Neuroeng.*, vol. 7, p. 26, Jul. 2014.

[11] G. R. Müller-Putz, I. Daly, and V. Kaiser, "Motor imagery-induced EEG patterns in individuals with spinal cord injury and their impact on brain-computer interface accuracy," *J. Neural Eng.*, vol. 11, no. 3, Sep. 2014, Art. no. 035011.

[12] S. Fazli *et al.*, "Enhanced performance by a hybrid NIRS-EEG brain computer interface," *Neuroimage*, vol. 59, no. 1, pp. 519–529, Jan. 2012.

[13] J. Herrera-Vega, C. G.Treviño-Palacios, and F. Orihuela-Espina, "Neuroimaging with functional near infrared spectroscopy: From formation to interpretation," *Infrared Phys. Technol.*, vol. 85, pp. 225–237, Sep. 2017.

[14] A. Salek-Haddadi, M. Merschhemke, L. Lemieux, and D. R. Fish, "Simultaneous EEG-correlated ictal fMRI," *Neuroimage.*, vol. 16, no. 1, pp. 32–40, May 2002.

[15] E. Visani *et al.*, "Hemodynamic and EEG time-courses during unilateral hand movement in patients with cortical myoclonus. An EEG-fMRI and EEG-TD-fNIRS study," *Brain Topogr.*, vol. 28, no. 6, pp. 915–925, Nov. 2015.

[16] S. C. Wriessnegger, D. Kirchmeyr, G. Bauernfeind, and G. R. Müller-Putz, "Force related hemodynamic responses during execution and imagery of a hand grip task: A functional near infrared spectroscopy study," *Brain Cognit.*, vol. 117, pp. 108–116 Oct. 2017.

[17] J. Hirsch, X. Zhang, J. A. Noah, and Y. Ono, "Frontal temporal and parietal systems synchronize within and across brains during live eye-to-eye contact," *Neuroimage*, vol. 157, pp. 314–330, Aug. 2017.

[18] H. Fujimoto *et al.*, "Neurofeedback-induced facilitation of the supplementary motor area affects postural stability," *Neurophotonics*, vol. 4, no. 4, Oct. 2017, Art. no. 045003.

[19] N. Naseer and K. S. Hong, "fNIRS-based brain-computer interfaces: A review," *Front. Hum. Neurosci.*, vol. 9, p. 3, Jan. 2015.

[20] M. A. Yücel, J. J. Selb, T. J. Huppert, M. A. Franceschini, and D. A. Boas, "Functional near infrared spectroscopy: Enabling routine functional brain imaging," *Curr. Opin. Biomed. Eng.*, vol. 4, pp. 78–86, Dec. 2017.

[21] J. Steinbrink, A. Villringer, F. Kempf, D. Haux, S. Boden, and H. Obrig, "Illuminating the BOLD signal: Combined fMRI-fNIRS studies," *Magn. Reson. Imag.*, vol. 24, no. 4, pp. 495–505, May 2006.

[22] S. B. Erdoğan, M. A. Yücel, and A. Akin, "Analysis of task-evoked systemic interference in fNIRS measurements-insights from fMRI," *Neuroimage*, vol. 87, pp. 490–504, Feb. 2014.

[23] V. Kaiser *et al.*, "Cortical effects of user training in a motor imagery based brain–computer interface measured by fNIRS and EEG," *Neuroimage*, vol. 85, pp. 432–444, Jan. 2014.

[24] V. Kaiser, A. Kreilinger, G. R. Müller-Putz, and C. Neuper, "First steps toward a motor imagery based stroke BCI: New strategy to set up a classifier," *Front. Neurosci.*, vol. 5, p. 86, Jul. 2011.

[25] R. Rupp, "Challenges in clinical applications of brain computer interfaces in individuals with spinal cord injury," *Front. Neuroeng.*, vol. 7, no. 7, p. 38, Sep. 2014.

[26] W. Yi *et al.*, "Enhancing performance of a motor imagery based brain-computer interface by incorporating electrical stimulation-induced SSSEP," *J. Neural Eng.*, vol. 14, no. 2, Apr. 2017, Art. no. 026002.

[27] X. Cui, S. Bray, and A. L. Reiss, "Functional Near Infrared Spectroscopy (NIRS) signal improvement based on negative correlation between oxygenated and deoxygenated hemoglobin dynamics," *Neuroimage*, vol. 49, no. 4, pp. 3039–3046, Feb. 2010.

[28] M. Mihara *et al.*, "Near-infrared spectroscopy-mediated neurofeedback enhances efficacy of motor imagery-based training in poststroke victims," *Stroke*, vol. 44, no. 4, pp. 1091–1098, Apr. 2013.

[29] M. J. Khan, M. J. Hong, and K. S. Hong, "Decoding of four movement directions using hybrid NIRS-EEG brain-computer interface," *Front. Hum. Neurosci.*, vol. 8, no. 1, p. 244, Apr. 2014.

[30] Y. Fu, X. Xin, C. Jiang, B. Xu, Y. Li, and H. Li, "Imagined hand clenching force and speed modulate brain activity and are classified by NIRS combined with EEG," *IEEE Trans. Neural Syst. Rehabil. Eng.*, vol. 25, no. 9, pp. 1641–1652, Sep. 2017.

[31] V. V. Nikulin *et al.*, "Monochromatic ultra-slow (~0.1 Hz) oscillations in the human electroencephalogram and their relation to hemodynamics," *Neuroimage*, vol. 97, pp. 71–80, Aug. 2014.

[32] A. M. Chiarelli, F. Zappasodi, F. D. Pompeo, and A. Merla, "Simultaneous functional near-infrared spectroscopy and electroencephalography for monitoring of human brain activity and oxygenation: A review," *Neurophotonics*, vol. 4, no. 4, p. 041411, Aug. 2017.

[33] S. Darvishi, A. Gharabaghi, C. B. Boulay, M. C. Ridding, D. Abbott, and M. Baumert, "Proprioceptive feedback facilitates motor imagery-related operant learning of sensorimotor β-band modulation," *Front. Neurosci.*, vol. 11, p. 60, Feb. 2017.

[34] H. Yuan, C. Perdoni, and B. He, "Relationship between speed and EEG activity during imagined and executed hand movements," *J Neural. Eng.*, vol. 7, no. 2, Feb. 2010, Art. no. 26001.

[35] R. Bauer, M. Fels, V. Royter, V. Raco, and A. Gharabaghi, "Closed-loop adaptation of neurofeedback based on mental effort facilitates reinforcement learning of brain self-regulation," *Clin. Neurophysiol.*, vol. 127, no. 9, pp. 3156–3164, Sep. 2016.

[36] F. Grimm, G. Naros, and A. Gharabaghi, "Compensation or restoration: Closed-loop feedback of movement quality for assisted reach-to-grasp exercises with a multi-joint arm exoskeleton," *Front. Neurosci.*, vol. 10, p. 280, Jun. 2016.

[37] S. Boe, A. Gionfriddo, S. Kraeutner, A. Tremblay, G. Little, and T. Bardouille, "Laterality of brain activity during motor imagery is modulated by the provision of source level neurofeedback," *Neuroimage*, vol. 101, pp. 159–167, Nov. 2014.

[38] K. J. Miller, G. Schalk, E. E. Fetz, M. D. Nijs, J. G. Ojemann, and R. P. Rao, "Cortical activity during motor execution, motor imagery, and imagery-based online feedback," *Proc. Natl. Acad. Sci.*, USA, vol. 107, no. 9, pp. 4430–4435, Mar. 2010.

[39] J. Feng *et al.*, "Towards correlation-based time window selection method for motor imagery BCIs," *Neural Netw.*, vol. 102, pp. 87–95, Jun. 2018.

[40] M. Xu, X. Xiao, Y. Wang, H. Qi, T. Jung, and D. Ming, "A brain-computer interface based on miniature-event-related potentials induced by very small lateral visual stimuli," *IEEE Trans. Biomed. Eng.*, vol. 65, no. 5, pp. 1166–1175, May 2018.